Energy Efficiency (2024) 17:23
https://doi.org/10.1007/s12053-024-10209-w

ORIGINAL ARTICLE

A numerical investigation of the influence of ozone on combustion to improve the performance of spark ignition engines

Marco D'Amato · Antonio Cantiani · Angelo Basso · Vinicio Magi · Annarita Viggiano

Received: 8 August 2023 / Accepted: 4 March 2024 / Published online: 13 March 2024

Abstract The aim of this work is to exploit the influence of using ozonized air to achieve stable and efficient combustion of lean mixtures in a gasoline-fuelled Spark-Ignition (SI) engine. The influence of ozone on the combustion of near-stoichiometric mixtures, which are typical of SI engines, has also been assessed. A Computational Fluid Dynamics (CFD) model has been employed to simulate compression, combustion, and expansion of a spark ignition, axisymmetric engine fuelled with iso-octane/air/ozone mixtures. The aim is to assess how ozone improves the engine performance under different engine speeds, ignition timings and equivalence ratios. The model has been validated against experimental data available in the literature. Parametric analyses have been carried out by considering three values of engine speeds (800, 1000 and 1200 rpm), three different ozone concentrations at Intake Valve Closure (IVC) (0, 100 and 200 ppm) and two equivalence ratios (0.9 and 0.7). The results show that ozone enables reactions in the Low Temperature Combustion (LTC) regime, modifies the mixture chemical composition and the auto-ignition tendency. Specifically, for all the cases under examination, the addition of ozone to the air/fuel mixture reduces the combustion duration, leading to an increase in terms of work output and a reduction of the specific fuel consumption. Moreover, the advantage of using ozone is greater for lean mixtures than for near-stoichiometric mixtures. Finally, for the near-stoichiometric cases, when the residence time of the mixture is high enough, auto-ignition occurs in the end gases.

Keywords Ozone · Combustion · Iso-octane · Spark Ignition Engine · Efficiency · CFD

M. D'Amato (✉) · A. Cantiani · A. Basso · V. Magi · A. Viggiano
School of Engineering, University of Basilicata, 85100 Potenza, Italy
e-mail: marco.damato@unibas.it

A. Cantiani
e-mail: antonio.cantiani@unibas.it

A. Basso
e-mail: angelo.basso001@studenti.unibas.it

V. Magi
e-mail: vinicio.magi@unibas.it

A. Viggiano
e-mail: annarita.viggiano@unibas.it

V. Magi
Department of Mechanical Engineering, San Diego State University, San Diego, CA 92182, USA

Introduction

Sustainability and energy efficiency are the key points to be pursued in an effort to reduce human impact on the environment. Most global greenhouse gas emissions come from the energy sector (over 73%) with a contribution from transport of about 16% (Ritchie et al., 2020). In the road transport sector, which is currently dominated by Internal Combustion Engines (ICEs), several strategies have been recently explored, including electric or hybrid vehicles, fuel cell electrical vehicles, the use of biofuels, and the adoption of unconventional thermal engines. The choice among the different solutions depends on several factors, such as consumer acceptance, political decisions, and specific applications. In any case, the combustion engine will continue to play a central role, whether it is used either for power generation or for transport.

Engineering research on ICEs needs to investigate technologies that are increasingly efficient in terms of both energy and environmental impact. An interesting recent technology is the use of ozone to enhance combustion (Sun et al., 2019). Indeed, a main feature of ozone is that, due to its relatively long lifetime (McClurkin & Maier, 2010), it can be used in the combustion region to promote fuel oxidation. Studies conducted on ozone assisted combustion have covered several aspects such as: mixture ignition (D'Amato, Magi, & Viggiano, 2022; Ji et al., 2017; Jiang et al., 2022; Nomaguchi & Koda, 1989; Xie et al., 2022), flame speed (D'Amato, Viggiano, & Magi, 2022; Gao et al., 2015; Halter et al., 2011; Ombrello et al., 2010; Wang et al., 2012), flame structure and stability (Ehn et al., 2015; Vu et al., 2014; Weng et al., 2015; Zhang et al., 2016). The addition of ozone influences several performance parameters of ICEs, such as ignition time control, Heat Release Rate (HRR), operating range, and pollutant emissions.

In the literature, most of the work on ozone-assisted combustion in internal combustion engines concerns with compression ignition engines (Foucher et al., 2013; Masurier et al., 2013; Masurier et al., 2015; Nishida & Tachibana, 2006; Pinazzi & Foucher, 2017a, 2017b; Yamada et al., 2005), where auto-ignition plays a key role. Specifically, main applications concern the improvement of combustion control of Homogeneous Charge Compression Ignition (HCCI) engines. Foucher et al. (2013) studied the influence of ozone in an n-heptane-fuelled HCCI engine, and observed that the addition of 50 ppm of O_3 was able to advance ignition by about 15 Crank Angle Degrees (CAD). Masurier et al. (2013) considered different Primary Reference Fuels (PRFs), from PRF0 to PRF100, and carried out experiments on a single cylinder of an HCCI engine. They showed that ozone promotes the formation of cool flames and advances the entire combustion process. Pinazzi and Foucher (2017a, 2017b) investigated the influence of ozone in a diesel engine operating under Partially Premixed Compression Ignition (PPCI) mode with direct gasoline injection. The authors found that the intake temperature, which should be high enough for gasoline auto-ignition and low-load operations, can be progressively reduced with the addition of ozone. Other studies examined the use of ozone in Spark Assisted Compression Ignition (SACI) engines (Biswas & Ekoto, 2019, 2020). Biswas and Ekoto (2019) have investigated the influence of ozone on the performance and emissions of a lean SACI engine. They found that ozone addition, by increasing the reactivity of the end gases, stabilizes combustion compared to the case without O_3.

Unlike Compression Ignition engines, only a few studies have investigated the use of ozone in Spark Ignition (SI) engines (Golke et al., 2023; Gong et al., 2018a, 2018b). Gong et al. (2018a, 2018b) carried out numerical investigations of an ozone-assisted, methanol-fuelled Direct Injection Spark Ignition (DISI) engine. The results show that the maximum in-cylinder pressure increases with ozone addition for both cold start and steady state modes. Golke et al. (2023) tested the addition of ozone as an ignition enhancer for a stoichiometric gasoline/ethanol blend diluted with residual gas to promote de-throttling, thus reducing part-load pumping losses. The results show that the engine efficiency can be increased with ozone addition, which enables combustion with a high residual gas fraction. However, the authors showed that ozone could favour autoignition of the end gases even at low compression ratio and residual gas fraction higher than 30%.

In this scenario, the aim of this work is to investigate the influence of ozone on a spark ignition engine fuelled with iso-octane, in order to understand, predict and provide guidance on the potential and limitations associated with ozone-assisted combustion for this type of engines. Since ozone reduces iso-octane ignition delay time, O_3 would promote detonation phenomena in conventional SI engines, under near-stoichiometric conditions, as shown by Golke et al. (2023). Instead, this work aims to assess whether the beneficial effect of ozone can be exploited when using lean mixtures in SI engines. Indeed, ozone makes the combustion process of lean mixtures faster and more efficient, while avoiding the autoignition phenomena that would occur under stoichiometric conditions.

On the other hand, by operating with leaner mixtures than those currently used, fuel savings and a reduction in emissions are achieved. Specifically, multi-dimensional CFD simulations have been carried out to evaluate the engine performances, considering different mixture compositions at IVC, engine speeds, and ignition timings. D'Amato, Cantiani, et al. (2022) investigated the influence of ozone on the Laminar Flame Speed (LFS) of an iso-octane/air/ozone mixture under spark ignition engine-like thermo-chemical conditions. Specifically, a CFD model has been used to simulate the compression stroke of an SI engine to compute the thermo-chemical conditions at the ignition timing. Then, such conditions have been used to calculate the LFS by means of a 1-D model. The results showed that ozone is able to significantly increase the LFS of the mixture, both under stoichiometric and lean conditions. Therefore, in this work, the influence of ozone on engine combustion is further studied by using a multi-dimensional CFD model to simulate the closed-valve working cycle of the engine. The aim is to assess the role of ozonized air in the combustion chamber, where fluid dynamics interacts with chemistry under turbulent regime.

This work is organized as follows: first, the model and the engine test-case are described, then the results of the simulations, concerning both the validation of the model and the influence of different operating parameters, are given, and, finally, main conclusions are summarized.

The CFD Model

Simulations have been carried out by using a multi-dimensional CFD model. Specifically, a Reynolds-Averaged Navier Stokes (RANS) approach is used, together with the standard $k-\varepsilon$ model for turbulence and wall functions for the near-wall treatment.

A kinetic mechanism is employed with 187 chemical species and 931 reactions. Such mechanism includes a sub-mechanism for iso-octane (Luong et al., 2013), a sub-mechanism for ozone (Halter et al., 2011) and a sub-mechanism for nitrogen oxides (Saxena & Williams, 2007). The kinetic mechanism has already been used and carefully discussed in Refs. (D'Amato, Cantiani, et al., 2022; D'Amato, Viggiano, & Magi, 2022). Specifically, the authors have used such mechanism to perform computations to evaluate the LFS of an iso-octane/air/ozone mixture. The mechanism has been validated by comparing the LFS with several experimental data, for different conditions of temperature, pressure, equivalence ratio and ozone concentration. A good agreement with measurements has been observed.

Transport equations are solved for each chemical species and turbulent combustion is simulated by employing the Eddy Dissipation Concept (EDC) model (Magnussen, 1981). The EDC model has already been successfully employed from several authors to study engines that operate under turbulent conditions with different combustion strategies, including spark ignition (Grimsmo & Magnussen, 1990) and compression ignition (D'Amato et al., 2020; Hong et al., 2008) engines.

The EDC combustion model assumes that the fluid can be separated into two regions: the chemical reactions take place in the first region, whereas the second region is non-reactive. Between the two regions, molecular mixing takes place. The source terms due to chemistry are modelled by taking into account the turbulence/chemistry interaction.

Simulations are carried out by using Fluent solver as a part of the Ansys® Academic Research CFD package, Release 20.2 (ANSYS, Inc., 2020).

The Engine Test-Case

The engine is a Port Fuel Injection (PFI) engine, which has been experimentally investigated by D'Errico et al., 2007. The experimental data, in terms of pressure and HRR as a function of crank angle, have been used to validate the numerical model by considering different values of the Spark Advance (SA). The engine specifications are given in Table 1.

A 2-D axisymmetric domain is used to significantly reduce the computational cost of the simulations when a detailed EDC combustion model is implemented. The combustion chamber geometry has already been employed in Cantiani et al. (2020), where a parametric analysis was carried out by varying the shape of the engine head with the aim of finding the geometry that is able to reproduce the experimental results. The computational domain is shown in Fig. 1. The grid is structured and uniform, except for the spark region (red colored region of Fig. 1). The numerical domain, at Intake Valve Closing (IVC), consists of 53,181 numerical cells and 53,671 grid points and has been

Table 1 Reference engine specifications

Displaced Volume	399 cc
Stroke	81.3 mm
Bore	79.0 mm
Connecting Rod	143.0 mm
Compression Ratio	10:1
Engine speed	1000 rpm
Intake Valve Closure (IVC)	144 CAD Before Top Dead Center (BTDC)
Exhaust Valve Open (EVO)	153 CAD After Top Dead Center (ATDC)

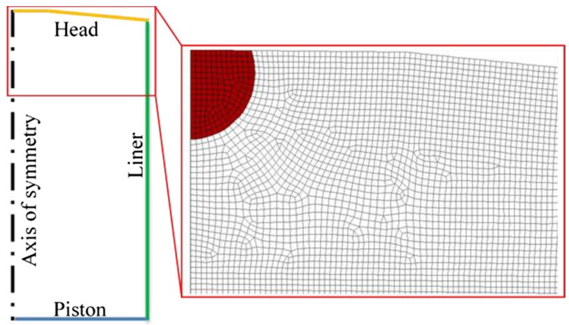

Fig. 1 Computational domain and a detail off the numerical grid

generated by using an average cell size equal to 0.25 mm. The resolution of the grid has been chosen to get proper values of y^+ along the wall boundaries for the use of standard wall functions.

The simulations start at IVC, i.e. at 144 CAD BTDC and end at Exhaust Valve Opening (EVO = 153 CAD ATDC). At IVC, a homogeneous mixture is considered, with iso-octane, air, ozone and residual gases (CO_2, H_2O, N_2 and O_2) from the previous work cycle. The composition of the residual gases is computed by considering a single global combustion reaction.

At ignition time, the gas mixture temperature in the spark region is artificially raised to 2800 K. Hence, a hot kernel develops and the flame front propagates in the chamber according to chemical kinetic and turbulent diffusion.

The initial and boundary conditions are given in Table 2. In the table, ozone concentration is evaluated

Table 2 Initial and boundary conditions of the simulations

Pressure at IVC	0.97 bar
Temperature at IVC	410 K
Wall temperature	430 K
Equivalence ratio	≃ 0.9, 0.7
Residual gas percentage	15%
Ozone concentration	0, 100, 200 ppm
Engine speed	800, 1000, 1200 rpm

with respect to the fresh intake mixture. The initial turbulent kinetic energy (k) and its dissipation rate (ε) have been estimated by using the expressions of Ref. (Viggiano & Magi, 2012).

An adaptive numerical time step is employed for accuracy. Specifically, a maximum time step, equal to 0.125 CAD, is used up to ignition and during late expansion, whereas, during ignition and combustion, the time step is reduced to 0.01 CAD.

Simulations of the closed-valve working cycle of the engine have been performed under different operating conditions. Specifically, the following engine parameters have been considered:

- three engine speeds (800, 1000, 1200 rpm), to assess the role of the mixture residence time when ozonized air is used;
- three ozone concentrations (0, 100, 200 ppm), to analyse the role of the amount of ozone on combustion;
- different spark ignition timings, in order to have the same CA50 (i.e. the crank angle corresponding to 50% of the total heat released) for different engine speeds, to analyse the influence of ozone when the thermodynamic efficiency of the working cycle is kept constant;
- a lean and a near-stoichiometric mixtures, to understand whether ozone is able to sustain lean combustion and to compare the engine performance with the near-stoichiometric case.

Results and discussion

Model validation

The model is validated by comparing the in-cylinder pressure and HRR profiles with experimental results available in the literature (D'Errico et al., 2007). In the experiments, the mixture is approximately stoichiometric. To account for both the engine blow-by, which reduces the fresh charge in the combustion chamber, and the crevices between piston and cylinder, where combustion is very inefficient, an equivalence ratio of 0.9 has been considered in the simulations. The engine speed is equal to 1000 rpm.

Since no experimental data with ozone are available in the literature, the model has been validated for an iso-octane/air mixture. However, the influence of ozone on the laminar flame speed of iso-octane has been extensively analysed in Ref. (D'Amato, Viggiano, & Magi, 2022) by using the same kinetic reaction mechanism employed in this work. The validation of the CFD model under turbulent conditions, even in the absence of ozone, is useful to assess the accuracy of the model in predicting turbulent flame speed.

The standard EDC model constants are used up to ignition, whereas, during combustion, the model constants have been adjusted to match measurements of Ref. (D'Errico et al., 2007). Specifically, the model constants for the fine-structures length fraction and the fine-structures characteristic time have been changed to 6.5 and 1.4, respectively.

Figure 2 shows a comparison between measurements and numerical simulations for different values of SA. As shown in Fig. 2(a), the model provides a very good agreement with the measured in-cylinder pressure profile, especially for the cases with earlier SA.

The highest discrepancies between experimental and numerical results have been observed just after TDC for the case with SA = 3 CAD BTDC, equal to 1.2 bar, and in the final stage of the expansion stroke, equal to 0.6 bar, as shown in Fig. 2(a). Combustion is also well predicted by the model, as shown in Fig. 2(c), where the comparison between the data available in Ref. (D'Errico et al., 2007) for the case with SA = 3 CAD BTDC and the numerical profile is given in terms of HRR. Some differences occur between TDC and 15 CAD ATDC, and just after the pressure peak value. However, since the experimental HRR profile is obtained from the in-cylinder pressure data on the basis of thermodynamic considerations, the validation can be considered more than satisfactory.

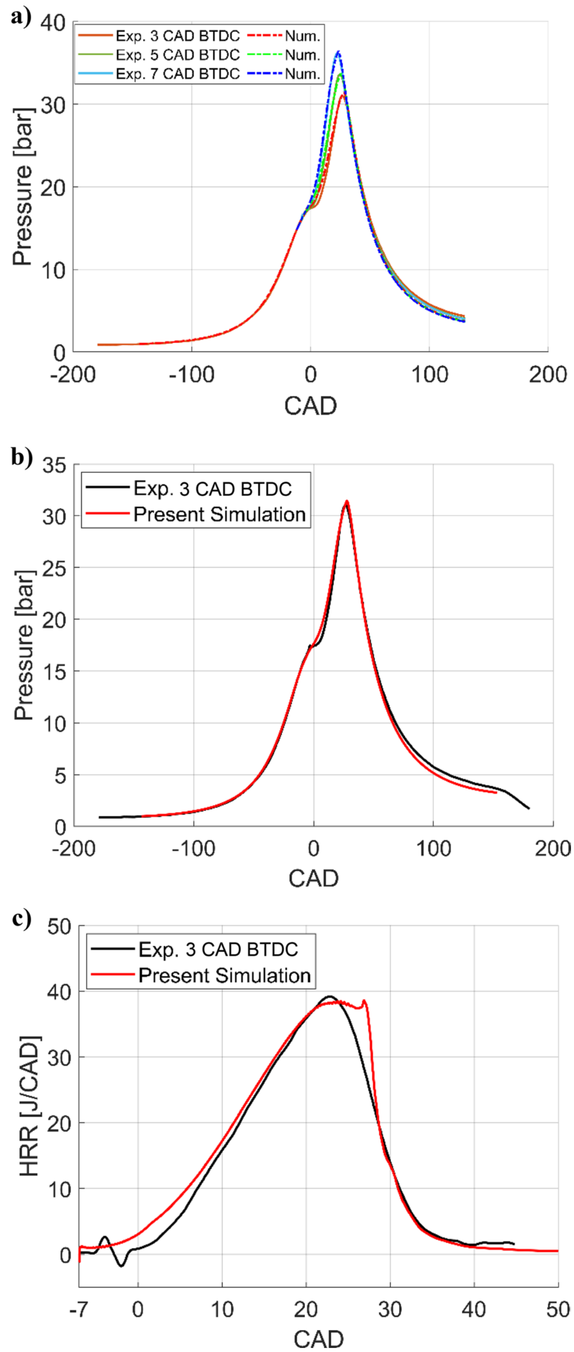

Fig. 2 Experimental and numerical results in terms of: (**a**) in-cylinder pressure for different values of SA; (**b**) in-cylinder pressure for SA = 3 CAD BTDC; (**c**) Heat Release Rate for SA = 3 CAD BTDC

In the following sections, the model setup based on the case with SA = 3 CAD BTDC will be used for further analyses.

Influence of ozone and parametric analysis

The influence of adding ozone to the fuel/air mixture at IVC is analysed by considering different ozone concentrations. Besides, a parametric analysis has been carried out by varying engine speed, equivalence ratio and SA, in order to evaluate the engine performance under different operating conditions. Specifically, the following engine parameters are evaluated: CA10; CA50; CA90 (i.e. the crank angle when 10%, 50% and 90% of the total heat has been released, respectively); the combustion duration (defined as the difference between CA90 and CA10); the maximum value of volume-averaged in-cylinder pressure, $\overline{P}_{MAX}$, computed as $\overline{P}_{MAX} = \max_{\theta}\left\{ \frac{1}{V}\int_V PdV \right\}$, and the crank angle, $\theta_{\overline{P}_{MAX}}$, at which this peak occurs; the gross indicated work per cycle, $W^g_{c,I}$, computed as $W^g_{c,I} = \int_{IVC}^{EVO} PdV$; the gross Indicated Mean Effective Pressure, $IMEP^g$, computed as $IMEP^g = \frac{W^g_{c,I}}{V_c}$; the gross Specific Fuel Consumption, SFC^g, computed as $SFC^g = \frac{M_{fuel_{IVC}}}{W^g_{c,I}}$, where $M_{fuel_{IVC}}$ is the fuel mass at IVC.

Engine speed and ozone concentration at fixed SA

Figure 3 shows the in-cylinder pressure profile without ozone and with the addition of 100 ppm O_3, with $\phi \simeq 0.9$ and for different engine speeds. The numerical SA is kept the same for all cases and equal to 7 CAD BTDC (-7 CAD). Table 3 shows the combustion parameters for the cases, whereas Table 4 summarizes the engine performance parameters.

The results show that, without ozone, the pressure peak shifts forward and decreases as engine speed increases. In addition, the gross indicated work per cycle decreases with a larger reduction for the 1200 rpm case. Indeed, as shown in Table 3, the combustion duration lasts longer and combustion occurs late during the expansion stroke as engine speed increases.

The addition of 100 ppm of ozone at IVC reduces the combustion duration for all the engine speeds, leading to an advance and increase of the pressure peak. Specifically, with the addition of 100 ppm of ozone, the combustion duration decreases by 43.25%, 28.87% and 20.79% for the 800, 1000 and 1200 rpm cases, respectively. With ozone addition, the gross indicated work per cycle increases for all the investigated engine speeds.

A further investigation has been carried out for the 800 rpm case, because the benefits of adding ozone at this speed are relatively small. Indeed, the excessive advance of the pressure peak results in a reduction of the pressure during the expansion stroke. Besides, Fig. 3 shows a sudden pressure increase with ozone addition at 800 rpm but also at 1000 rpm, suggesting that auto-ignition of the fresh mixture occurs.

The Maximum Pressure Rise Rate (MPRR) has been computed to address this tendency. Specifically, for the 800 rpm case without ozone, the MPRR is equal to 1.21 bar/CAD and occurs at 14.82 CAD ATDC, i.e. before 50% of the total heat has been released, and the pressure peak occurs at +23.63 CAD. Furthermore, starting from CA50, 40% of the total heat is released in about 8 CAD (CA90-CA50). For the case with 100 ppm of ozone, the MPRR increases to 17.98 bar/CAD and occurs at 13.24 CAD ATDC, i.e. close to the pressure peak. The significant increase of the MPRR is due to the faster heat release in the second part of combustion: CA50-CA10 is equal to about 8 CAD, whereas CA90-CA50 is only 2 CAD. This acceleration leads to a rapid increase in temperature and, therefore, in pressure. The auto-ignition of the mixture is also shown in Fig. 4, where the in-cylinder temperature distribution is given, for the cases with and without ozone and for different engine speeds, at 13 CAD ATDC. The flame front has swept a larger chamber volume for the cases with ozone addition. At 13 CAD ATDC, a larger amount of fresh mixture is burned for the lowest engine speed case. As shown in the figure, for the 800 rpm case with 100 ppm of ozone, the fresh mixture auto-ignites in the region between the flame front and the cylinder walls, leading to a sudden pressure increase.

Such auto-ignition is due to the presence of ozone, which enables chemical reactions in the LTC regime, leading to the production of radicals, as shown in Fig. 5, and reducing the Ignition Delay Time (IDT) of the mixture. These auto-ignition phenomena occur earlier the lower the engine speed, because the residence time of the mixture is longer. If the residence time is small, auto-ignition occurs either later or does not occur at all. Specifically, for

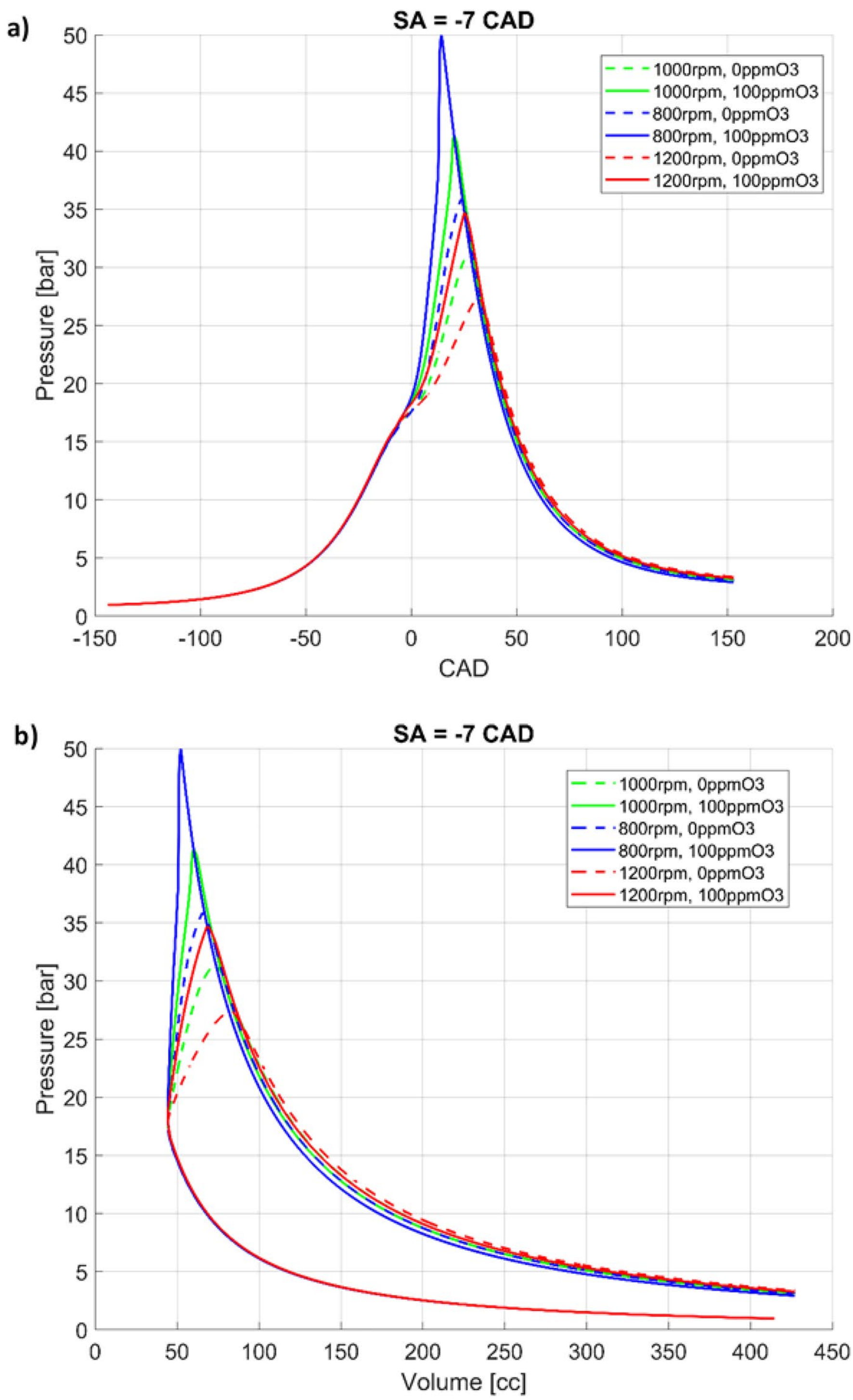

Fig. 3 In-cylinder pressure profiles for different engine speeds at $\phi = 0.9$, with and without ozone, and with SA = 7 CAD BTDC: (**a**) pressure as a function of CAD; (**b**) pressure as a function of volume chamber

the 800 rpm case, auto-ignition occurs at about 12.8 CAD ATDC and about 60% of the total heat has already been released; for the 1000 rpm case, auto-ignition occurs at about 19 CAD ATDC and 78% of the total heat has already been released; for the 1200 rpm case, auto-ignition does not occur.

Figure 5(a) shows the in-cylinder hydroperoxyl (HO_2) mass fraction distribution, which characterizes

Table 3 Combustion parameters for different engine speeds at $\phi = 0.9$, with and without ozone, and with SA = 7 CAD BTDC

$Value_{0ppm_{O_3}}$ / $Value_{100ppm_{O_3}}$			
Parameter	800rpm	1000rpm	1200rpm
CA10 [CAD]	+6.56 / +3.47	+8.22 / +5.31	+9.77 / +7.01
CA50 [CAD]	+16.88 / +11.70	+20.37 / +15.22	+24.07 / +18.65
CA90 [CAD]	+25.01 / +13.94	+29.35 / +20.34	+33.77 / +26.02
CA90-CA10 [CAD]	18.45 / 10.47	21.13 / 15.03	24.00 / 19.01
$\overline{P}_{MAX}$ **[bar]**	35.85 / 49.96	31.44 / 41.29	27.45 / 34.70
$\theta_{\overline{P}_{MAX}}$ **[CAD]**	+23.63 / +14.24	+27.67 / +20.31	+31.88 / +25.29

Table 4 Engine performance parameters for different engine speeds at $\phi = 0.9$, with and without ozone, and with SA = 7 CAD BTDC

$Value_{0ppm_{O_3}} / \frac{Value_{100ppm_{O_3}} - Value_{0ppm_{O_3}}}{Value_{0ppm_{O_3}}} * 100$			
Parameter	800rpm	1000rpm	1200rpm
$W^g_{c,I}$ **[J]**	286.76 / +0.86%	285.01 / +3.34%	280.07 / +4.47%
$IMEP^g$ **[bar]**	7.20 / +0.86%	7.15 / +3.34%	7.03 / +4.47%
SFC^g **[g/kWh]**	212.8 / -0.86%	214.1 / -3.24%	217.9 / -4.29%

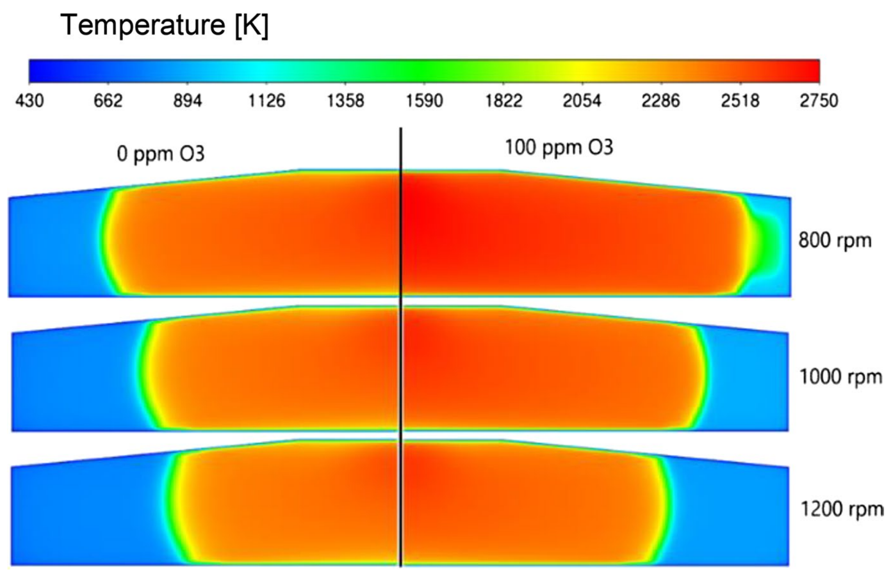

Fig. 4 In-cylinder temperature distribution at 13 CAD ATDC, without ozone (left) and with 100 ppm of ozone (right) at $\phi = 0.9$, with SA = 7 CAD BTDC, for different engine speeds

the LTC regime, at 5 CAD BTDC for the 1200 rpm case with and without ozone. Figure 5(b) shows the HO_2 values along an axis perpendicular to the flame front. For the case without ozone, HO_2 is produced only in the region already swept by the flame front, with a peak in the flame preheating region. Instead. with ozone addition, HO_2 is produced throughout the chamber, even in areas away from the flame. During the compression stroke, ozone decomposition produces oxygen atoms, thus modifying the fuel reaction pathways. Radicals and intermediate species accelerate chemical kinetics, resulting in an increase of flame speed and temperature in the "unburnt gas" region, as shown in Fig. 6, where the in-cylinder temperature is given at 15 CAD ATDC for the 1200 rpm with and without ozone cases.

For the 1000 rpm case, simulations have also been carried out by adding 200 ppm of ozone at IVC. Figure 7 shows the pressure and HRR profiles obtained by different ozone concentrations. As expected,

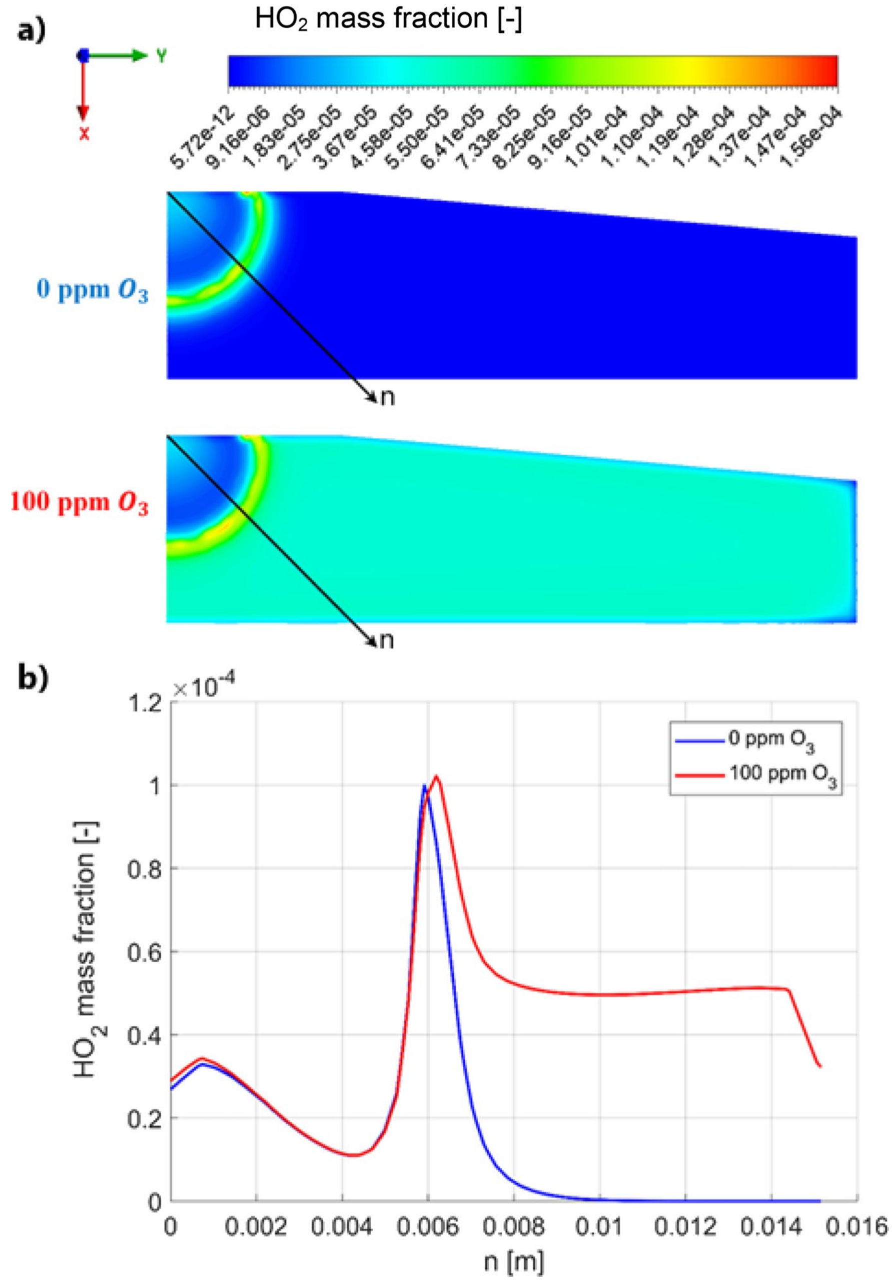

Fig. 5 In-cylinder HO_2 mass fraction at 5 CAD BTDC with and without ozone at $\phi = 0.9$ and 1200 rpm: (**a**) HO_2 mass fraction contour plot; (**b**) HO_2 mass fraction value along the n-axis

and as shown by both pressure and HRR profiles, by increasing ozone concentration, combustion is advanced and the onset of auto-ignition is promoted, as suggested by the sudden increase of HRR in Fig. 7(c). As summarized in Table 5, with 200 ppm of ozone, CA50 advances by 2.05 CAD with respect to the case with 100 ppm, whereas the combustion duration (CA90-CA10) is equal to 12.05 CAD, which is 9.08 CAD and 2.98 CAD less than the cases without ozone and with 100 ppm of ozone, respectively. The pressure peak occurs at 16.4 CAD ATDC with a value of 47.35 bar; the MPRR is 13.03 bar/s and occurs at 15.3 CAD ATDC.

The very early pressure peak, due to the early auto-ignition in the end gases, results in a faster pressure decrease during the expansion stroke due to an increase of heat transferred to the walls. Hence, there is no additional work gain with respect to the 100

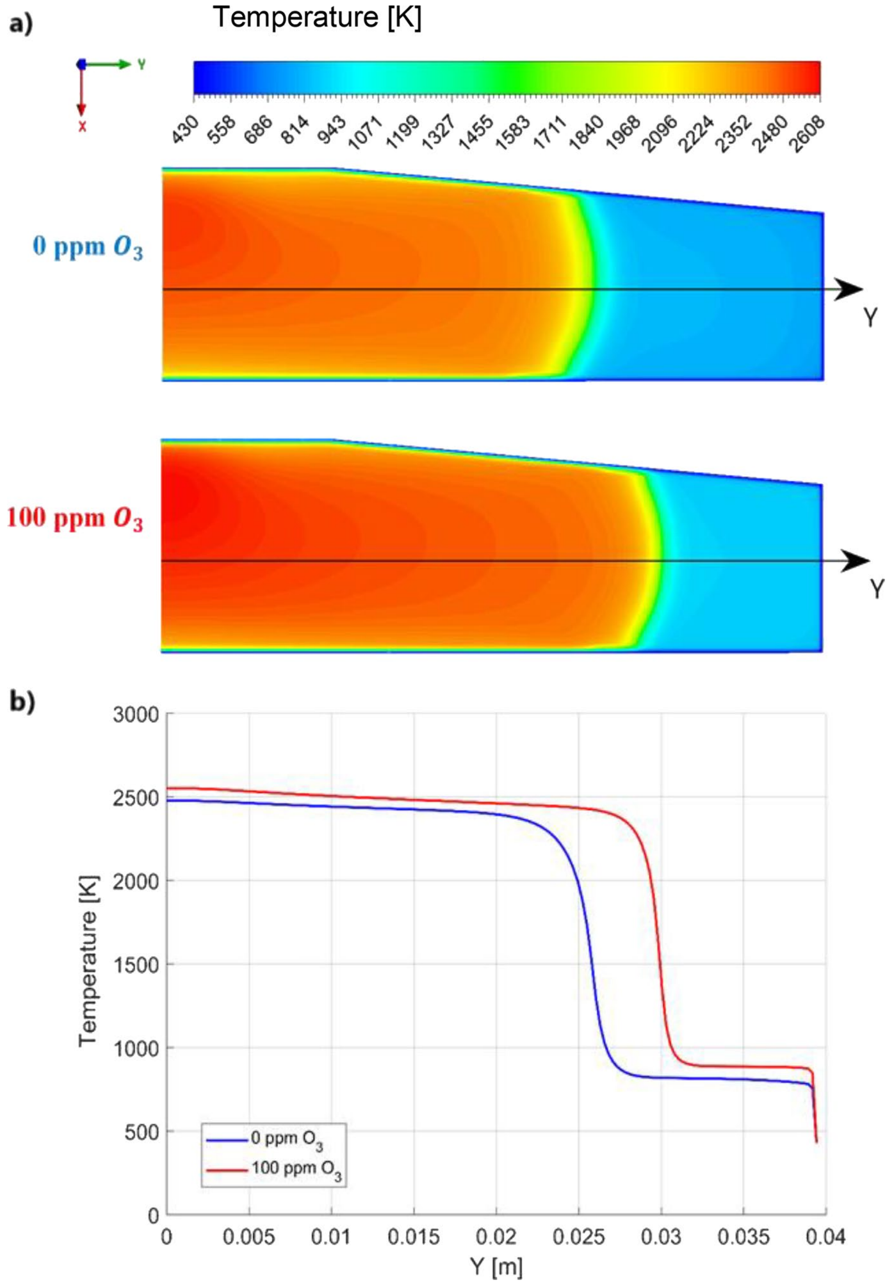

Fig. 6 In-cylinder temperature at 15 CAD ATDC with and without ozone at $\phi = 0.9$ and 1200 rpm: (**a**) temperature distribution; (**b**) temperature value along the Y axis

ppm case. Specifically, the gross indicated work per cycle, $W^g_{c,I}$ and $IMEP^g$ increase by 3.36% compared to the case without ozone, which is similar to the benefit obtained for the 100 ppm case.

Furthermore, the influence of ozone on emissions has been assessed by comparing the results obtained for cases without O_3 and with ozonated air. Specifically, with respect to the case without ozone, CO_2 is almost unchanged and CO decreases by 51% and 73% with 100 and 200 ppm of O_3, respectively. On the other hand, NO_x concentration in the exhaust gas, which is 2590 ppm for the case without ozone, increases by 40% and 76% with the addition of 100 and 200 ppm of ozone, respectively. Both the reduction of CO and the increase of NO_x depend on the increase of the in-chamber temperature as ozone concentration increases, as shown in Fig. 4 and in Fig. 6, and on the auto-ignition phenomenon promoted by

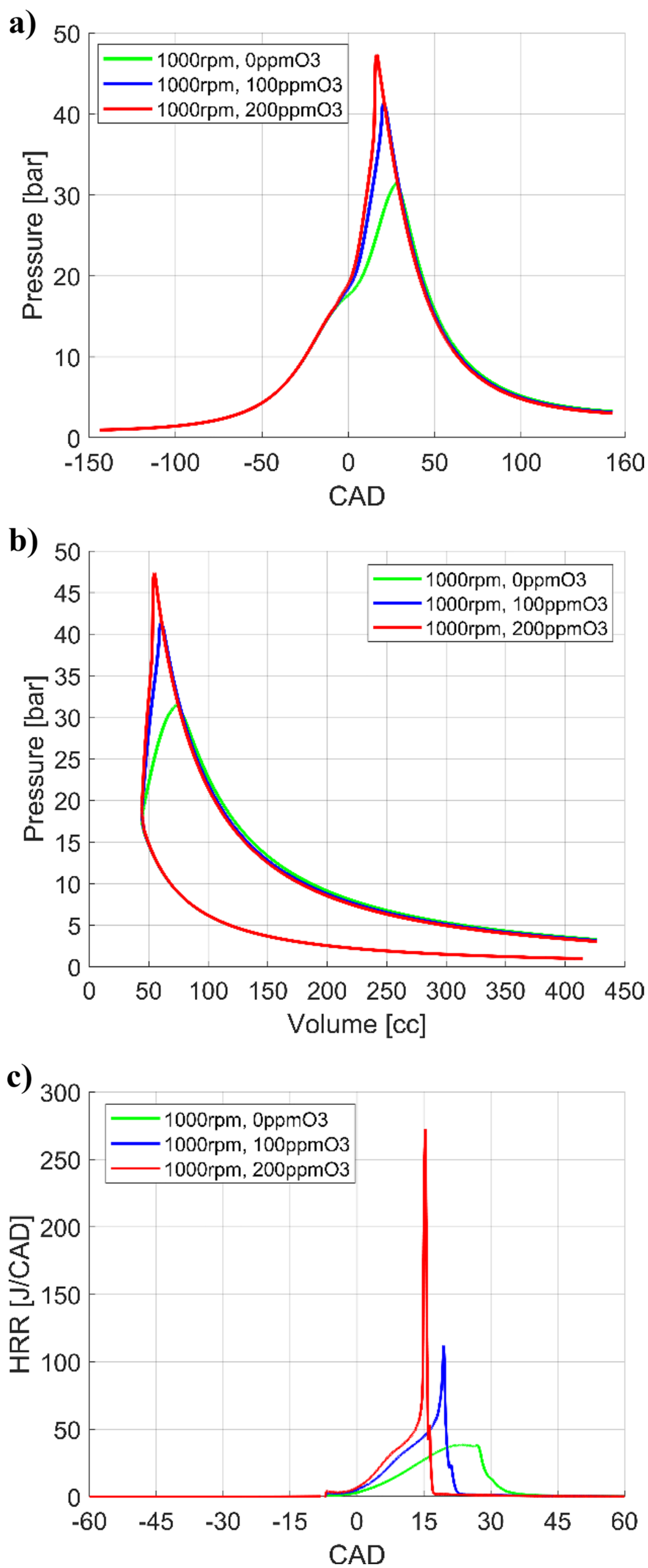

Fig. 7 Pressure and HRR profiles obtained by varying ozone concentrations with SA = 7 CAD BTDC at $\phi = 0.9$ and 1000 rpm: (**a**) pressure as a function of CAD; (**b**) pressure as a function of volume; (**c**) HRR

Table 5 Combustion parameters for different ozone concentrations at 1000 rpm, ϕ=0.9, and with SA = 7 CAD BTDC

Parameter	0 ppm_{O_3}	100 ppm_{O_3}	200 ppm_{O_3}
CA10 [CAD]	+8.22	+5.31	+3.93
CA50 [CAD]	+20.37	+15.22	+13.17
CA90 [CAD]	+29.35	+20.34	+15.98
CA90-CA10 [CAD]	21.13	15.03	12.05
$\overline{P}_{MAX}$ **[bar]**	31.44	41.29	47.35
$\theta_{\overline{P}_{MAX}}$ **[CAD]**	+27.67	+20.31	+16.4

ozone, which in turn leads locally to a significant increase of temperature.

Engine speed and ozone concentration at fixed CA50

Simulations without ozone have been carried out at different engine speeds by changing SA, in order to have approximately the same CA50 of the baseline case (1000 rpm; CA50 = 20 CAD ATDC). Specifically, for 800 rpm SA is equal to 5 CAD BTDC and for 1200 rpm SA is equal to 9 CAD BTDC.

The same SA and the corresponding engine speed have also been employed with ozone. Figure 8 shows the results in terms of pressure profiles for the cases without ozone and with the addition of 100 ppm of O_3 for different engine speeds. Tables 6 and 7 show the combustion and the engine performance parameters for the different cases.

Without ozone, at the same CA50, both the value of peak pressure and the relative crank angle are comparable to the case with ozone, with differences lower than 1 bar and 1 CAD, respectively. $W^g_{c,I}$increases with the engine speed, since expansion in the engine is faster and the wall heat transfer reduces: for the 800 rpm case, the average temperature at the end of the expansion stroke is 1332 K, whereas, for the 1200 rpm case, is 1382 K. With the addition of 100 ppm ozone, as for the cases with constant SA, combustion is faster and shorter, and this is more pronounced by reducing the engine speed. Ozone enables to increase the engine performance, with a benefit that varies from +2.9% for the 800 rpm case to +3.34% for the 1000 rpm case, in terms of $W^g_{c,I}$. However, auto-ignition of the mixture in the end gases occurs for all cases with ozone. Specifically, for the 800 rpm case, auto-ignition occurs at about 16.1 CAD ATDC, when about 64% of the total heat has already been released; for the 1200 rpm case, auto-ignition occurs at about 20.75 CAD ATDC, when about 81% of the total heat has already been released.

Influence of ozone on a lean mixture

As previously shown, by reducing iso-octane IDT, ozone can promote detonation phenomena for conventional SI engines, which operate under stoichiometric conditions. This result was also found by Golke et al. (2023), who used gasoline/ethanol stoichiometric mixtures diluted with exhaust gases. The innovative contribution of this work is to analyse whether the addition of ozone is able to provide stable combustion of lean mixtures, which are characterized by longer IDT. Under lean conditions, ozone beneficial effect could be exploited by avoiding, at the same time, the autoignition phenomena that would occur by using near-stoichiometric mixtures. This is a very interesting result as by operating with leaner mixtures than those currently employed, fuel savings and a reduction in emissions are achieved.

The influence of ozone on a lean mixture, i.e. $\phi \simeq 0.7$, has been investigated at 1000 rpm. Simulations have been carried out by using both the same SA, equal to 7 CAD BTDC, as for the baseline case (1000 rpm without ozone), and the same CA50 as for the baseline case, which is obtained by advancing SA to 11 CAD BTDC. Cases without ozone and with 100 ppm ozone have been considered. Tables 8 and 9 show the combustion and performance parameters for such cases, whereas Fig. 9 shows the pressure profiles and heat release rate as a function of CAD. Finally, Fig. 10 shows a comparison between the cases with different equivalence ratios, in terms of pressure profiles as a function of volume in the closed-valve working cycle. For the lean mixture case, the total heat released is lower than for the near-stoichiometric case, due to the lower amount of fuel in the chamber, and the work output is lower as well. However, a comparison can be made based on the specific fuel consumption, SFC^g.

The results show that, for the case with SA = 7 CAD BTDC and without ozone, combustion proceeds very slowly. Indeed, CA50 and CA90 are 32.85 CAD ATDC and 53.43 CAD ATDC, respectively, and the combustion duration is 42.35 CAD. The peak pressure rises over the pressure at TDC by only 0.7 bar, resulting in an increase of the specific

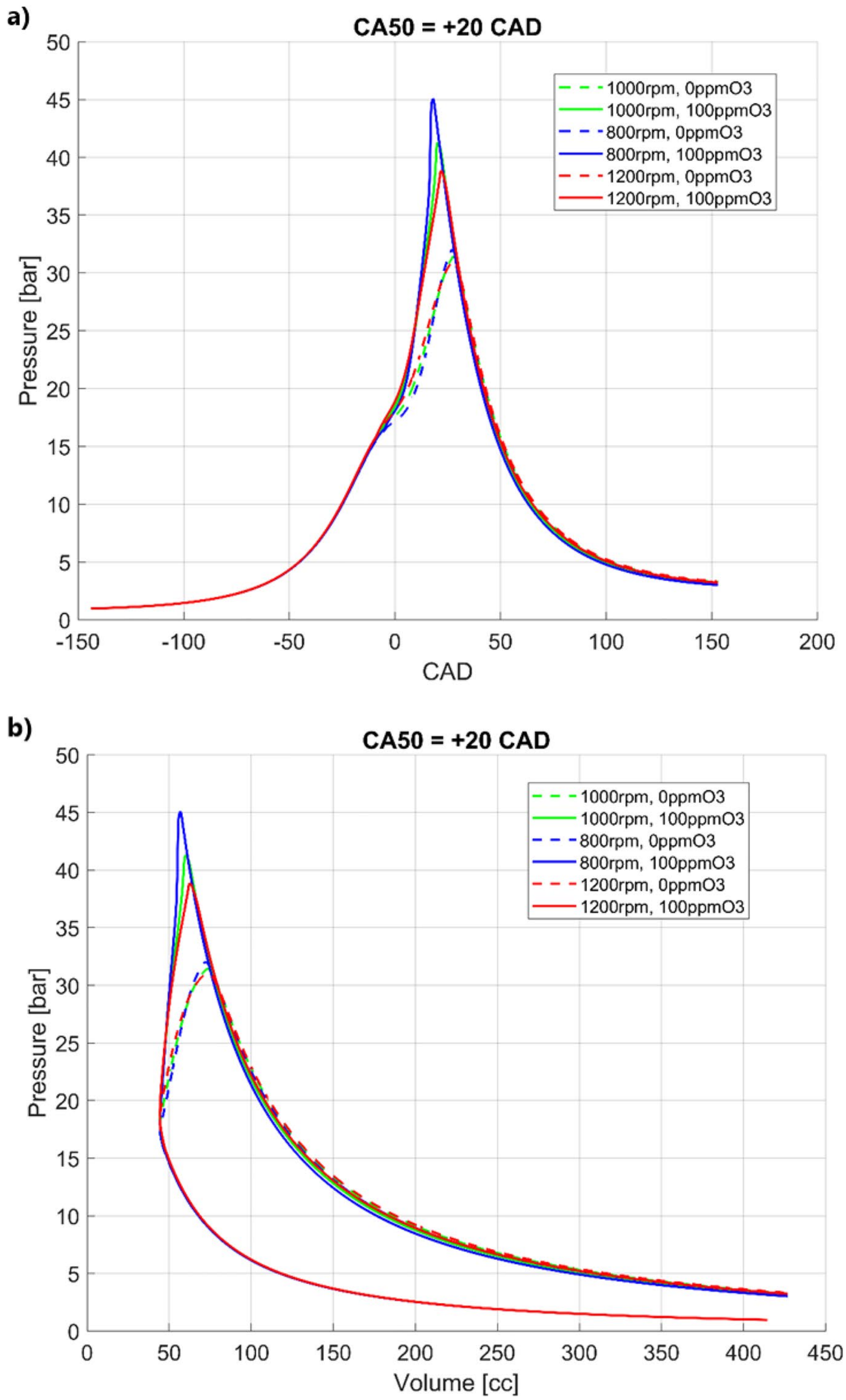

Fig. 8 Pressure profiles for different engine speeds, with and without ozone at $\phi = 0.9$, and with CA50 $\simeq$ 20 CAD ATDC without ozone: (**a**) pressure as a function of CAD; (**b**) pressure as a function of volume

fuel consumption and, therefore, in a loss of work compared to the case with SA = 11 CAD BTDC, as shown in Fig. 10 and Table 9.

For cases with ozone, higher engine performances are obtained, as shown in Table 9. Specifically, with the addition of 100 ppm of O_3, the gross work per

Table 6 Combustion parameters for different engine speeds, with and without ozone at $\phi = 0.9$, and with CA50 ≃ 20 CAD ATDC without ozone

$\text{Value}_{0ppm_{O_3}}$ / $\text{Value}_{100ppm_{O_3}}$			
Parameter	800rpm	1000rpm	1200rpm
CA10 [CAD]	+9.10 / +5.63	+8.22 / +5.31	+7.3 / +4.79
CA50 [CAD]	+20.32 / +14.37	+20.37 / +15.22	+20.29 / +15.71
CA90 [CAD]	+28.83 / +17.65	+29.35 / +20.34	+29.61 / +22.28
CA90-CA10 [CAD]	19.73 / 12.02	21.13 / 15.03	22.31 / 17.49
$\overline{P}_{MAX}$ **[bar]**	32.02 / 45.08	31.44 / 41.29	31.12 / 38.85
$\theta_{\overline{P}_{MAX}}$ **[CAD]**	+27.07 / +18.00	+27.67 / +20.31	+28 / +21.90

Table 7 Engine performance parameters for different engine speed, with and without ozone at $\phi = 0.9$, and with CA50 ≃ 20 CAD ATDC without ozone

$\text{Value}_{0ppm_{O_3}} / \frac{\text{Value}_{100ppm_{O_3}} - \text{Value}_{0ppm_{O_3}}}{\text{Value}_{0ppm_{O_3}}} * 100$			
Parameter	800rpm	1000rpm	1200rpm
$W^g_{c,I}$ **[J]**	280.72 / +2.9%	285.01 / +3.34%	288.7 / +3.17%
$IMEP^g$ **[bar]**	7.04 / +2.9%	7.15 / +3.34%	7.24 / +3.17%
SFC^g **[g/kWh]**	217.4 / -2.83%	214.1 / -3.24%	211.4 / -3.08%

Table 8 Combustion parameters at 1000 rpm and $\phi = 0.7$, with and without ozone

$\text{Value}_{0ppm_{O_3}}$ / $\text{Value}_{100ppm_{O_3}}$		
Parameter	SA=-7 CAD	SA=-11 CAD
CA10 [CAD]	+11.08 / +7.53	+6.05 / +3.11
CA50 [CAD]	+32.85 / +20.70	+21.51 / +14.11
CA90 [CAD]	+53.43 / +29.00	+30.02 / +19.50
CA90-CA10 [CAD]	42.35 / 21.47	23.97 / 16.39
$\overline{P}_{MAX}$ **[bar]**	18.39 / 27.31	26.37 / 36.73
$\theta_{\overline{P}_{MAX}}$ **[CAD]**	+11.69 / +28.4	+28.87 / +19.63

Table 9 Engine performance parameters at 1000 rpm and $\phi = 0.7$, with and without ozone

$\text{Value}_{0ppm_{O_3}} / \frac{\text{Value}_{100ppm_{O_3}} - \text{Value}_{0ppm_{O_3}}}{\text{Value}_{0ppm_{O_3}}} * 100$		
Parameter	SA=-7 CAD	SA=-11 CAD
$W^g_{c,I}$ **[J]**	202.62 / +13.5%	230.6 / +4.17%
$IMEP^g$ **[bar]**	5.08 / +13.5%	5.78 / +4.17%
SFC^g **[g/kWh]**	235.28 / -11.9%	206.73 / -4.02%

cycle increases by 13.5% and 4.17%, whereas the combustion duration decreases by 49.3% and 31.62% for the cases with SA =7 CAD BTDC and SA = 11 CAD BTDC, respectively. Indeed, ozone enables LTC reactions and leads to both a slight increase in the end gases temperature, and to the production of radicals that promote the flame propagation. This results in a more pronounced influence of ozone for the cases where combustion is slower and more difficult to self-sustain.

For the case with SA = 11 CAD BTDC, which has approximately the same CA50 as the baseline case with $\phi = 0.9$, the lower equivalence ratio results in a small increase of the combustion duration, which is 23.97 CAD and 21.13 CAD for $\phi = 0.7$ and $\phi = 0.9$, respectively. However, compared to the case without ozone, combustion duration with ozone is reduced by 7.58 CAD and 6.1 CAD for the $\phi = 0.7$ and $\phi = 0.9$ cases, respectively. These results are in good agreement with those obtained in Ref. (D'Amato, Viggiano, & Magi, 2022). Specifically, with the same ozone concentration, a lower equivalence ratio leads to a reduction of LFS, but to a greater percentage increase of LFS compared to the case without ozone.

For the lean case, unlike the case with $\phi = 0.9$, the addition of 100 ppm of ozone does not lead to auto-ignition of the mixture, for both SA = 7 CAD BTDC and SA = 11 CAD BTDC, since the low equivalence ratio leads to an increase of the ignition delay time, which is longer than the residence time of the end gases.

As regards emissions, the addition of 100 ppm O_3 leads to a decrease of CO in the exhaust gases, with respect to the case without ozone, by 90% and 63% for the lean cases with SA = 7 CAD BTDC and SA = 11 CAD BTDC, respectively. On the other hand, without ozone, the exhaust NO_x concentration is equal to 73 ppm and 246 ppm for the cases with SA

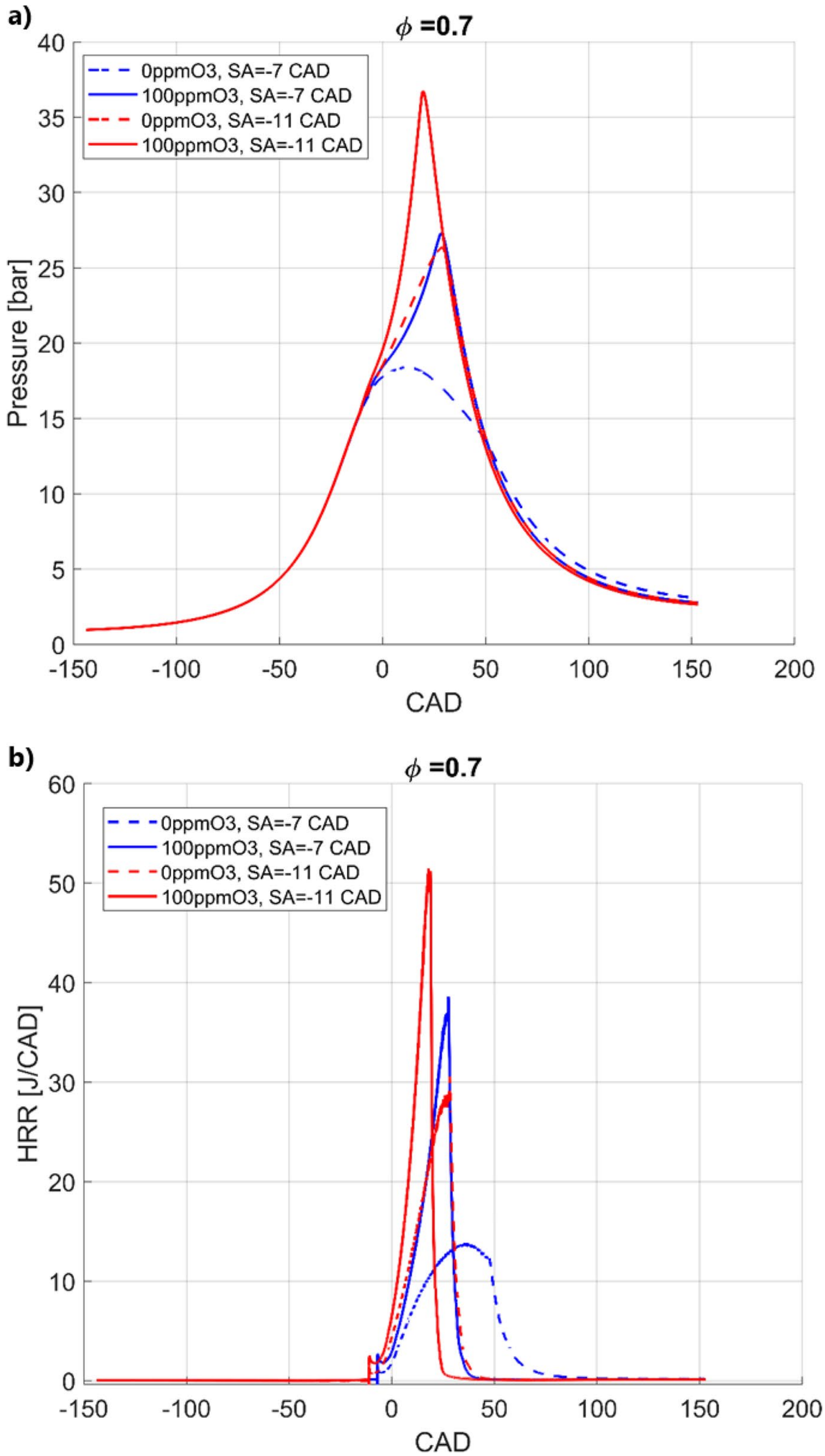

Fig. 9 Pressure (**a**) and Heat Release Rate (**b**) as a function of CAD with different ozone concentrations and SA, at 1000 rpm with $\phi = 0$

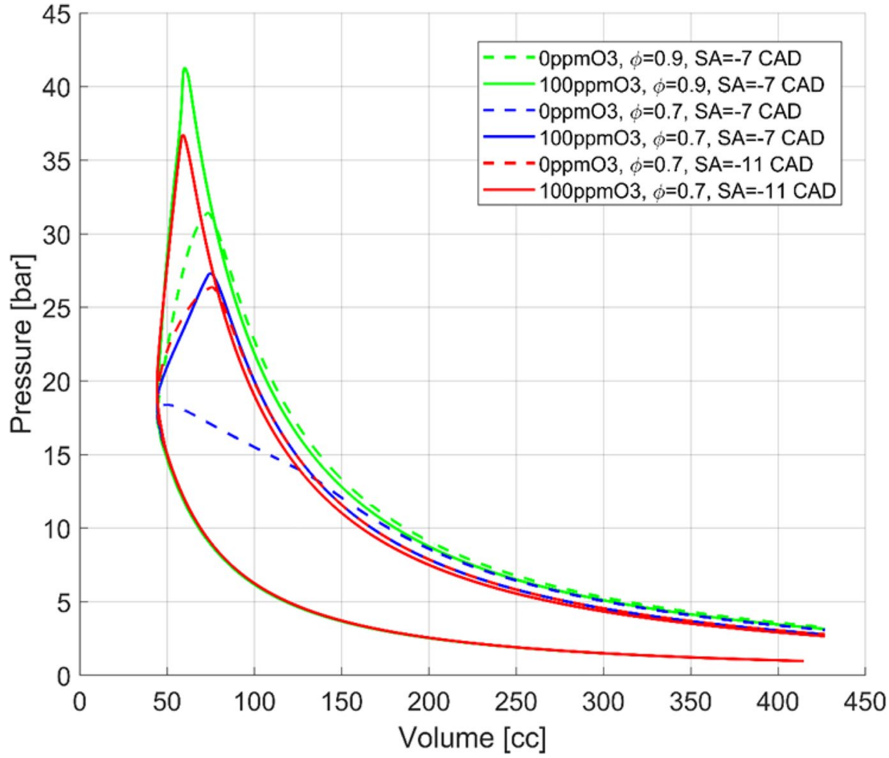

Fig. 10 Pressure as a function of volume chamber at 1000 rpm, for different ozone concentrations, equivalence ratios and SA

= 7 CAD BTDC and SA = 11 CAD BTDC, respectively, whereas with the addition of 100 ppm O_3 increases to 255 and 650 ppm, respectively. Without ozone and with SA = 7 CAD BTDC, the flame propagates very slowly, so the temperature in the chamber is lower, which explains both the considerable reduction of CO and the significant increase of NO_x when ozone-assisted combustion is used.

However, lean mixtures have benefits in terms of NO_x and CO_2 compared to the near-stoichiometric case, since less fuel is used and combustion temperature is lower. Specifically, comparing the near-stoichiometric case with the lean case at the same thermodynamic efficiency (i.e. at the same CA50), CO_2 emission for $\phi=0.7$ is about 77% of that for $\phi=0.9$. On the other hand, by adding 100 ppm of ozone in the lean case, NO_x emission is about 4 times lower than that of the near-stoichiometric case without ozone.

Furthermore, to assess the influence of ozone on CO_2, it is useful to consider the ratio between the mass of CO_2 in the exhaust gases and the gross-indicated work per cycle for each case. For $\phi=0.9$, CO_2 emission is reduced from 808 g/kWh to 782 g/kWh moving from 0 to 100 ppm O_3. For the same ozone concentrations, but for the cases with $\phi=0.7$, CO_2 emission decreases from 875 g/kWh to 773 g/kWh when SA is set to 3 CAD BTDC, and from 770 g/kWh to 740 g/kWh when SA is modified to keep the same CA50 of the baseline case. These results suggest that ozone-assisted combustion is extremely attractive when using lean mixtures, because in addition to increasing combustion efficiency, emissions can be significantly reduced.

Conclusions

In this work, the influence of ozone on the performance of a spark ignition engine has been investigated by considering near-stoichiometric and lean mixture conditions in order to provide guidance for future applications of ozone-assisted combustion. Multi-dimensional CFD simulations of the closed-valve cycle of an axisymmetric engine fuelled with iso-octane/air/ozone mixtures have been carried out. The model has been validated by comparing the pressure and heat release profiles against experimental data available in the literature. Simulations have been carried out by considering different engine speeds, by keeping constant either SA or CA50.

The main findings can be summarized as follows:

- ozone addition results in faster flame propagation, which is more pronounced the longer the residence time of the mixture;
- a delay of SA and a lower engine speed provide more time for the ozone to deplete and allow reactions in the Low-Temperature Combustion regime. This occurs both during the compression stroke and in the end gases, leading to an increase of the flame speed;
- for the near-stoichiometric cases, when the residence time of the mixture is long enough, autoignition of end gases generally occurs. Further studies are needed in order to select engine operating conditions that guarantee a residence time lower than the IDT of the unburned mixture, to avoid auto-ignition for stoichiometric cases;
- for all cases, the addition of ozone results in an increase of the gross indicated work per cycle and a reduction of the specific fuel consumption. However, for cases with near-stoichiometric mixtures, when auto-ignition occurs, the numerical result may overestimate the actual engine performance;
- for lean cases, the flame speed benefits more from ozone addition with respect to the near-stoichiometric cases. Indeed, the gross indicated work per cycle increases by 4% and 14% for the near-stoichiometric and lean cases, respectively. Furthermore, auto-ignition does not occur when lean mixtures are used;
- ozone promotes the reduction of fuel consumption and pollutant emissions by operating with leaner mixtures than those currently used in SI engines.

A further development of this work is the use of ozone to optimize the combustion of fuels other than gasoline (e.g. sustainable fuels, such as e-fuels and bio-fuels). Indeed, such fuels are currently being investigated to meet the requirements of a carbon neutral energy and propulsion system.

Acknowledgements This research was funded by MIUR - “Ministero dell’Istruzione, dell’Università e della Ricerca”, “Fondo Europeo di Sviluppo Regionale”, “PON Ricerca e Innovazione 2014-2020”, under project EXTREME, ARS01_00849.

Funding Open access funding provided by Università degli Studi della Basilicata within the CRUI-CARE Agreement.

Data Availability Data sets generated during the current study are available from the corresponding author on reasonable request.

Declarations

Conflict of interest The authors declare no competing interests.

References

Ansys® Academic Research CFD, Release 20.2, ANSYS, Inc. (2020). https://www.ansys.com/academic/terms-and-conditions

Biswas, S., & Ekoto, I. (2019). *Detailed Investigation into the Effect of Ozone Addition on Spark Assisted Compression Ignition Engine Performance and Emissions Characteristics*. SAE Tech. Paper 2019-01-0966. https://doi.org/10.4271/2019-01-0966

Biswas, S., & Ekoto, I. (2020). Ozone Added Spark Assisted Compression Ignition. In A. Singh, N. Sharma, R. Agarwal, & A. Agarwal (Eds.), *Advanced Combustion Techniques and Engine Technologies for the Automotive Sector. Energy, Environment, and Sustainability*. Springer. https://doi.org/10.1007/978-981-15-0368-9_8

Cantiani, A., Viggiano, A., & Magi, V. (2020). *A CFD Model of Supercritical Water Injection for ICEs as Energy Recovery System*. SAE Tech. Paper 2020-37-0001. https://doi.org/10.4271/2020-37-0001

D’Amato, M., Cantiani, A., Magi, V., & Viggiano, A. (2022). The Laminar Flame Speed of Iso-Octane/Air/Ozone Lean Mixtures under Engine-Like Thermo-chemical Conditions. *IOP Conference Series: Earth and Environmental Science, 1106*. https://doi.org/10.1088/1755-1315/1106/1/012005

D’Amato, M., Magi, V., & Viggiano, A. (2022). On Iso-octane Combustion with Ozone Addition under HCCI Engine-Like Conditions. *Journal of Physics: Conference Series, 2385*, 012086. https://doi.org/10.1088/1742-6596/2385/1/012086

D'Amato, M., Viggiano, A., & Magi, V. (2020). On the Turbulence-Chemistry Interaction of an HCCI Combustion Engine. *Energies, 13*(22), 5876. https://doi.org/10.3390/en13225876

D'Amato, M., Viggiano, A., & Magi, V. (2022). A numerical investigation on the laminar flame speed of methane/air and iso-octane/air mixtures with ozone addition. *Combustion and Flame, 241*, 112145. https://doi.org/10.1016/j.combustflame.2022.112145

D'Errico, G., et al. (2007). *Development and Experimental Validation of a Combustion Model with Detailed Chemistry for Knock Predictions*. SAE Tech. Paper 2007-01-0938. https://doi.org/10.4271/2007-01-0938

Ehn, A., et al. (2015). Plasma assisted combustion: Effects of O3 on large scale turbulent combustion studied with laser diagnostics and Large Eddy Simulations. *Proceedings of the Combustion Institute, 35*(3), 3487–3495. https://doi.org/10.1016/j.proci.2014.05.092

Foucher, F., Higelin, P., Mounaïm-Rousselle, C., & Dagaut, P. (2013). Influence of ozone on the combustion of n-heptane in a HCCI engine. *Proceedings of the Combustion Institute, 34*(2), 3005–3012. https://doi.org/10.1016/j.proci.2012.05.042

Gao, X., et al. (2015). The effect of ozone addition on laminar flame speed. *Combustion and Flame, 162*(10), 3914–3924. https://doi.org/10.1016/j.combustflame.2015.07.028

Golke, D., et al. (2023). Potential of ozone addition on dethrottling of a gasoline/ethanol blend-fueled direct injection spark ignition engine in part load. *International Journal of Engine Research, 24*(6), 2523–2537. https://doi.org/10.1177/14680874221123611

Gong, C. M., et al. (2018). Numerical analysis of carbon monoxide, formaldehyde and unburned methanol emissions with ozone addition from a direct-injection spark-ignition methanol engine. *Energy, 144*, 432–442. https://doi.org/10.1016/j.energy.2017.12.068

Gong, C. M., et al. (2018). Numerical study of plasma produced ozone assisted combustion in a direct injection spark ignition methanol engine. *Energy, 153*, 1028–1037. https://doi.org/10.1016/j.energy.2018.04.096

Grimsmo, B., & Magnussen, B. F. (1990). *Numerical Calculation of Turbulent Flow and Combustion in an Otto Engine Using the Eddy Dissipation Concept*. Proceedings of the Comodia 90. 3–5 September 1990.

Halter, F., Higelin, P., & Dagaut, P. (2011). Experimental and Detailed Kinetic Modeling Study of the Effect of Ozone on the Combustion of Methane. *Energy & Fuels, 25*(7), 2909–2916. https://doi.org/10.1021/ef200550m

Hong, S., et al. (2008). Modeling of Diesel Combustion, Soot and NO Emissions Based on a Modified Eddy Dissipation Concept. *Combustion Science and Technology, 180*(8), 1421–1448. https://doi.org/10.1080/00102200802119340

Ji, S., et al. (2017). Influence of Ozone on Ignition and Combustion Performance of a Lean Methane/Air Mixture. *Energy & Fuels, 31*(12), 14191–14200. https://doi.org/10.1021/acs.energyfuels.7b02389

Jiang, C., et al. (2022). Effects of mixing ozone on combustion characteristics of premixed methane/oxygen in meso-scale channels. *Fuel, 312*, 122792. https://doi.org/10.1016/j.fuel.2021.122792

Luong, M. B., et al. (2013). Direct numerical simulations of the ignition of lean primary reference fuel/air mixtures with temperature inhomogeneities. *Combustion and Flame, 160*(10), 2038–2047. https://doi.org/10.1016/j.combustflame.2013.04.012

Magnussen, B. F. (1981). *On the structure of turbulence and a generalized Eddy Dissipation Concept for chemical reaction in turbulent flow*. Proceedings of the 19th Aerospace Sciences Meeting. 12–15 January 1981.

Masurier, J.-B., Foucher, F., Dayma, G., & Dagaut, P. (2013). Homogeneous charge compression ignition combustion of primary reference fuels influenced by ozone addition. *Energy & Fuels, 27*(9), 5495–5505. https://doi.org/10.1021/ef401009x

Masurier, J.-B., Foucher, F., Dayma, G., & Dagaut, P. (2015). Ozone applied to the homogeneous charge compression ignition engine to control alcohol fuels combustion. *Applied Energy, 160*, 566–580. https://doi.org/10.1016/j.apenergy.2015.08.004

McClurkin, J., & Maier, D. (2010). *Half-life time of ozone as a function of air conditions and movement*. Proceedings of the 10th International Working Conference on Stored Product Protection. https://doi.org/10.5073/jka.2010.425.167.326

Nishida, H., & Tachibana, T. (2006). Homogeneous charge compression ignition of natural gas/air mixture with ozone addition. *Journal of Propulsion and Power, 22*, 151–157. https://doi.org/10.2514/1.14991

Nomaguchi, T., & Koda, S. (1989). Spark ignition of methane and methanol in ozonized air. *Symposium (International) on Combustion, 22*(1), 1677–1682. https://doi.org/10.1016/S0082-0784(89)80180-8

Ombrello, T., Won, S. H., Ju, Y., & Williams, S. (2010). Flame propagation enhancement by plasma excitation of oxygen. Part I: effects of O3. *Combustion and Flame, 157*(10), 1906–1915. https://doi.org/10.1016/j.combustflame.2010.02.005

Pinazzi, P. M., & Foucher, F. (2017). Influence of Injection Parameters, ozone seeding and residual NO on a Gasoline Compression Ignition (GCI) engine at low load. *Proceedings of the Combustion Institute, 36*(3), 3659–3668. https://doi.org/10.1016/j.proci.2016.06.075

Pinazzi, P. M., & Foucher, F. (2017). *Potential of Ozone to Enable Low Load Operations of a Gasoline Compression Ignition (GCI) Engine*. SAE Tech. Paper 2017-01-0746. https://doi.org/10.4271/2017-01-0746

Ritchie, H., Roser, M., & Rosado, P. (2020). *CO2 and Greenhouse Gas Emissions*. Published online at OurWorldInData.org., Retrieved January 2023., from https://ourworldindata.org/co2-and-other-greenhouse-gas-emissions

Saxena, P., & Williams, F. A. (2007). Numerical and Experimental Studies of Ethanol Flames. *Proceedings of the Combustion Institute, 31*(1), 1149–1156. https://doi.org/10.1016/j.proci.2006.08.097

Sun, W., Gao, X., Wu, B., & Ombrello, T. (2019). The effect of ozone addition on combustion: Kinetics and dynamics. *Progress in Energy and Combustion Science, 73*, 1–25. https://doi.org/10.1016/j.pecs.2019.02.002

Viggiano, A., & Magi, V. (2012). A comprehensive investigation on the emissions of ethanol HCCI engines. *Applied*

Energy, 93, 277–287. https://doi.org/10.1016/j.apenergy.2011.12.063

Vu, T. M., Won, S. H., Ombrello, T., & Cha, M. S. (2014). Stability enhancement of ozone-assisted laminar premixed Bunsen flames in nitrogen co-flow. *Combustion and Flame, 161*(4), 917–926. https://doi.org/10.1016/j.combustflame.2013.09.023

Wang, Z. H., et al. (2012). Investigation of combustion enhancement by ozone additive in CH4/air flames using direct laminar burning velocity measurements and kinetic simulations. *Combustion and Flame, 159*(1), 120–129. https://doi.org/10.1016/j.combustflame.2011.06.017

Weng, W., et al. (2015). Investigation of formaldehyde enhancement by ozone addition in CH4/air premixed flames. *Combustion and Flame, 162*(4), 1284–1293. https://doi.org/10.1016/j.combustflame.2014.10.021

Xie, W., Drost, S., Schebl, R., & Maas, U. (2022). *Preprint SSRN*. https://papers.ssrn.com/sol3/papers.cfm?abstract_id=4109908. Accessed January 2023 .

Yamada, H., Yoshii, M., & Tezaki, A. (2005). Chemical mechanistic analysis of additive effects in homogeneous charge compression ignition of dimethyl ether. *Proceedings of the Combustion Institute, 30*(2), 2773–2780. https://doi.org/10.1016/j.proci.2004.08.253

Zhang, Y., et al. (2016). Ozone effect on the flammability limit and near-limit combustion of syngas/air flames with N2, CO2, and H2O dilutions. *Fuel, 186*, 414–421. https://doi.org/10.1016/j.fuel.2016.08.094